JOURNAL OF ENZYME INHIBITION AND MEDICINAL CHEMISTRY
2018, VOL. 33, NO. 1, 1335–1342
https://doi.org/10.1080/14756366.2018.1493472

Taylor & Francis
Taylor & Francis Group

RESEARCH PAPER

Rapidly screening of α-glucosidase inhibitors from *Dioscorea opposita* Thunb. peel based on rGO@Fe_3O_4 nanocomposites microreactor

Songsong Zhang[a,b], Beibei Qiu[a,b], Jinhua Zhu[a,b], Weiping Hu[a,b], Fanyi Ma[a,b], M. Z. H. Khan[a,b,c] and Xiuhua Liu[a,b]

[a]College of Chemistry and Chemical Engineering, Henan University, Kaifeng, China; [b]Key Laboratory of Natural Medicine and Immune-Engineering of Henan Province, Henan University, Kaifeng, China; [c]Department of Chemical Engineering, Jessore University of Science and Technology, Jessore, Bangladesh

ABSTRACT

Present study aimed to immobilise the α-glucosidase on suitable supports to construct enzymatic microreactors and their subsequent applicability in efficient inhibitor screening from the Chinese Yam (*Dioscorea opposita* Thunb.) peel. A type of lamellar and porous composites (rGO@Fe_3O_4) were synthesised with a facile one-step solvothermal method and employed as carriers to construct enzymatic microreactors for screening α-glucosidase ligand from the Chinese Yam peel in league with the high performance liquid chromatography and mass spectrometry (HPLC-MS). The immobilisation amount of α-glucosidase on rGO@Fe_3O_4 under the optimised conditions was about 40 μg α-glucosidase/mg carriers. Furthermore, the binding capacities of screened inhibitors, 2,4-dimethoxy-6,7-dihydroxyphenanthrene and batatasin I, were 35.6 and 68.2%, respectively. Hence, considering their high screening efficiency and excellent magnetic separation ability, these as-prepared nanocomposite consisting of rGO and Fe_3O_4 may be potential supports for the enzyme (such as α-glucosidase) immobilisation for rapid α-glucosidase inhibitors screening from the diverse nature resources.

ARTICLE HISTORY
Received 11 April 2018
Revised 7 June 2018
Accepted 21 June 2018

KEYWORDS
rGO@Fe_3O_4 nanocomposite; enzymatic microreactors; α-glucosidase inhibitors; Chinese Yam (*Dioscorea opposita* Thunb.)

Introduction

Type 2 diabetes mellitus (T2DM), mainly manifested as disorder of glucose metabolism, obesity, etc. is a kind of multifactorial disease and chronic metabolic diseases that influenced by gene defect, surrounding environments and living ways with insulin resistance and hyposecretion of insulin[1–3]. α-glucosidase, a group of membrane-bound enzyme in the intestinal epithelial cells, hydrolyzes the substrates (starch, sucrose, etc.) that contain glucosidic linkage to release the glucose and then leads to the postprandial blood glucose increasing effect[4], thus the reversible inhibition effect of α-glucosidase was one of the approaches currently used to improving the glucose metabolism imbalances and fat abnormalities conditions[5]. Turkish reseachers identified that four medicinal herbs, concluding *Urtica dioica*, *Taraxacum officinale*, *Viscum album*, and *Myrtus communis*, showed high α-glucosidase inhibitor activity, the inhibitor activities different according to different α-glucosidase origins, and *Myrtus communis* (IC_{50} =38 μg/mL) could be developed as a new type of physiologically functional drink for lowing the blood glucose content[6]. Matsumura *et al.*[7] found that the water-soluble extract from leaves of *Eugenia uniflora L.* (*Myrtaceae*) could highly inhibited the α-glucosidase and proved by sucrose tolerance test (STT), glucose tolerance test (GTT) in mice experiments, α-glucosidase inhibition assay, and could provide some useful informations for the design of α-glucosidase ligand medicines. The crude extracts from fresh tuberous rhizomes of *Dioscorea opposita* Thunb. (Chinese Yam) were studied against yeast α-glucosidase that showed strong inhibitory activities and *trans-N-p*-coumaroyltyramine (IC_{50}=0.40 μM) was isolated from the *Dioscoreaceae* family for the first time in our previous work[8].

Bioactivity-guided screening has been one of mainstream methods to discover active natural products[9–13]. Two active components (6-*O*-(*p*-coumaroyl)-*D*-glucopyranoside, methyl 6-*O*-(*p*-coumaroyl)-β-*D*-galactopyranoside) were identified and purified from Tinta Cão grape pomace extract with bioactivity-guided fractionation methods that strongly inhibited intestinal α-glucosidase, and could be the potential development of a novel anti-hyperglycaemic drugs[14]. Bioactivity- guided screening by free enzymes could supply the useful information whether the complex natural resources inhibited corresponding enzyme, but this method continued to have a serious problem, lack of inhibitors separation ability, so immobilising the enzymes on solid substrates (such as nanoparticle, nanocomposite, etc.) to construct enzyme microreactors was a effective method that contained the advantages of separation ability and the highly sensitivity of bioactivity-guided screening method. Human serum albumin (HSA) functionalised by magnetic nanoparticle (MNPs) to construct HSA-MNPs were employed to successfully separate three saponins (dioscin, gracillin, and *pseudo*-protodioscin) from *D. nipponica* extract and showed strongly affinity with HSA, and this work present a easy and effective method to separated inhibitors from complex medicinal plants[15]. Lipase-Fe_3O_4 magnetic nanoparticle conjugates (LMNPs) were developed based on ligand fishing method and effectively supplied to isolate quercetin-3-*O*-β-D-arabinopyranosyl-(1 → 2)-β-D-galactopyranoside and quercetin-3-*O*-β-D-glucuronide from lotus (*Nelumbo nucifera* Gaertn.) leaf extract that widely used in China for weight-loss foods, and this method showed great power for rapidly lipase inhibitors screening from edible and medicinal plants[16]. Tao *et al.*[17] developed a method using α-glucosidase-functionalised magnetic bead by covalent linkage to

CONTACT Jinhua Zhu Zhu zhujinhua0528@163.com; Xiuhua Liu liuxiuhua@henu.edu.cn College of Chemistry and Chemical Engineering, Henan University, Kaifeng 475004, China

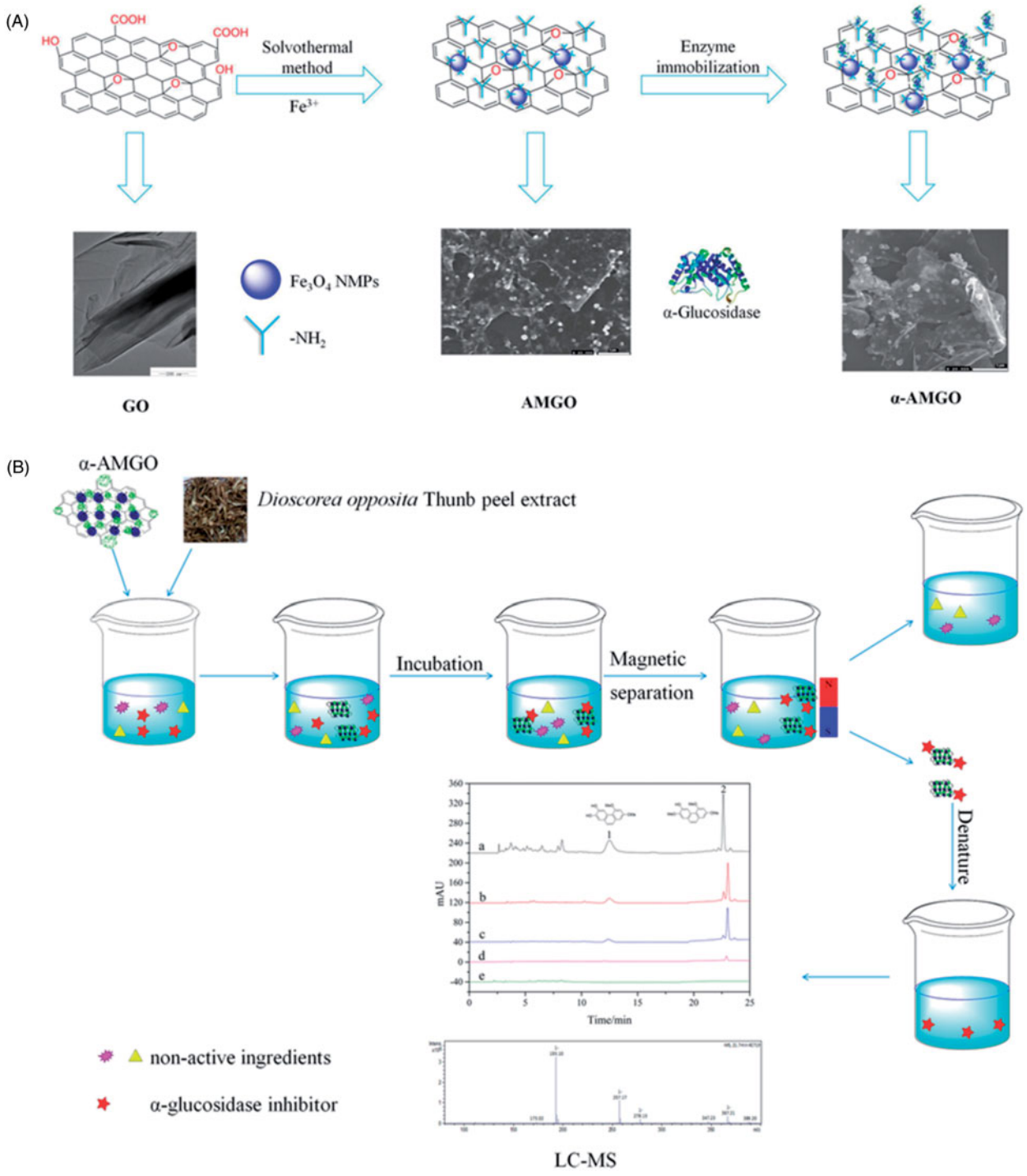

Figure 1. The synthesis procedure of AMGO nanocomposites, and α-AMGO microreactors (A) and the application schematic diagram (B) of the α-glucosidase microreactors in this experiment.

screen the enzyme inhibitors from *Morus alba* extract and successfully separated two flavonoids (isoquercitrin and astragalin), and their work demonstrated that enzyme-functionalised magnetic beads method might be applicable for discovering the active compounds in complex medicinal plants.

This work was to develop a facile and effective method to synthesise biocompatible nanocomposite, and then employed them as solid substrates to immobilise the α-glucosidase for the construction of α-glucosidase microreactors for the screening experiments of α-glucosidase inhibitors from Chinese Yam (*Dioscorea opposita* Thunb.) peel. The free NH_2 groups on the biocompatible nanocomposite were ideal reaction sites for the functionlisation of α-glucosidase with the typical glutaraldehyde (GA) activation process by the generation of Schiff base. The construction diagrammatic illustration was shown in Figure 1. The application schematic diagram of the α-glucosidase microreactors in this experiment was shown in Figure 2. The results of this work demonstrated that rGO@Fe_3O_4 biocompatible nanocomposite prepared by one-pot solvothermal method are promising supports to achieve higher immobilisation efficiency and binding capacities.

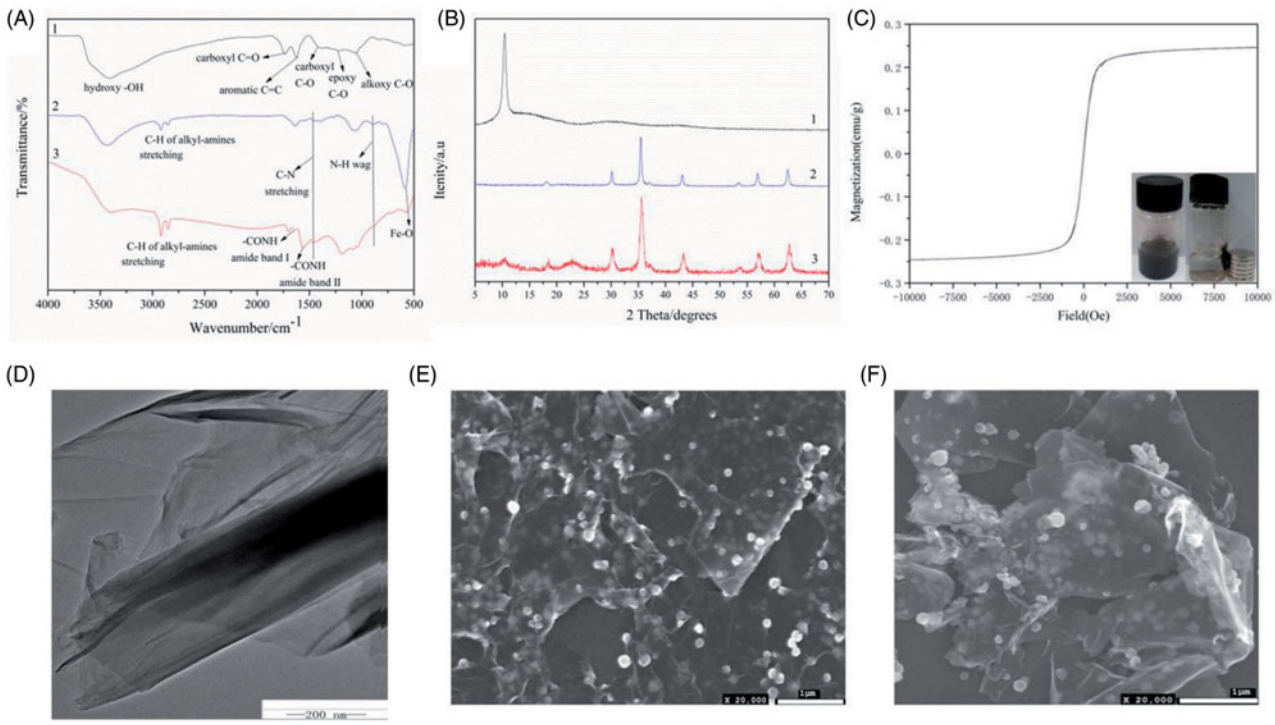

Figure 2. FT-IR spectra (A) of the GO (1), NH_2-Fe_3O_4 (2), AMGO (3). Powder X-ray diffractogram (B) of GO (1), NH_2-Fe_3O_4 (2) and AMGO nanocomposites (3). Room-temperature magnetisation curves (C) of AMGO nanocomposites. The inset picture in (C) showed the AMGO dispersibility and magnetic separation ability. TEM images of GO (D). SEM images of AMGO at 2.5:1 (E) and α-AMGO microreactors (F).

Materials and methods

Materials

Grapheme oxide (GO) (100602, Nanjing XFnano Materials Tech Co., Ltd. China); $FeCl_3{\cdot}6H_2O$ (analytically pure, Aladdin Chemistry Co., Ltd. China); α-glucosidase from Saccharomyces cerevisiae (EC 3.2.1.20, Sigma-Aldrich Chemical, St. Louis, MO); 4-nitrophenyl-α-D-glucopyranoside (pNPG) (98%, J&K Scientific Ltd. China); *Dioscorea opposita* Thunb. (Huai Shan Yao) was obtained from Jiaozuo city (Henan, China) in 2016 where it is famous of planting Huai Shan Yao for more than 1000 years. The voucher specimens (No. SYP20161116) of yam were stored in our lab which is in college of chemistry and chemical engineering, Henan University; batatasin I and 2,4-dimethoxy-6,7-dihydroxyphenanthrene were provided by our group[8,18–20]. All other solvents in this research were used as received without further purification.

Apparatus

1260 HPLC (Agilent Technologies Co., Ltd, MA); AmaZon SL ion trap mass spectrometry (Bruker Daltonik GmbH Co., Ltd, Bremen); 5C18-PAQ (4.6 (ID) × 250 (mm)) chromatography column (Cosmosil, Japan); incubator (QYC-2102C, CIMO Instrument Manufacturing Co., Ltd. Shanghai, China); microplate reader (DNM-9606, Perlong Medical Equipment Co., Ltd. Beijing, China); D8 Advance XRD characterisation (Bruker, Germany); JSM-7610F scanning electron microscope (JEOL Ltd. Japan); MPMS3 Magnetic properties (Quantum Design); VERTEX 70 infrared spectra (Bruker, Germany); JEM-2100 transmission electron microscope (JEOL Ltd. Japan).

Preparation of AMGO biocompatible nanocomposite

Amine-functionalised rGO@Fe_3O_4 (AMGO) nanocomposite were synthesised by a facile one-step solvothermal method using ethylene glycol (30.00 ml), anhydrous sodium acetate (0.5000 g), 1,6-hexanediamine (1.625 g) and $FeCl_3{\cdot}6H_2O$ (0.2500 g) as solvent, dispersing agent, nitrogen precursor and ferric source, respectively, combined with GO (0.1000 g) at 198 °C with a reaction time of 6 h. Finally, black products were washed by water and ethyl alcohol in ultrasonic condition to remove solvents and excessive 1,6-hexanediamine successfully, and then dried at 45 °C under vacuum and then stored in 4 °C for next characterisation and use. The synthesis diagrammatic illustration of biocompatible nanocomposite was shown in Figure 1(A).

Construction of α-glucosidase microreactors

The α-glucosidase was covalent interaction with the amino group of AMGO nanocomposite by employing glutaraldehyde (GA) as the crosslinking agent[18–21] to construct α-glucosidase microreactors (α-AMGO). The synthesis and construction diagrammatic illustration were shown in Figure 1(A). There were some parameters, including proportion of $FeCl_3{\cdot}6H_2O$ to GO (w/w), glutaraldehyde concentration, immobilised time and enzyme amount, need to be optimised to obtain the optimal construction conditions of α-glucosidase microreactors. The ultimate α-glucosidase amount immobilised on AMGO nanocomposite surfaces was computed according to our previous work[19,22]. Finally, α-AMGO microreactors were stored in phosophate-buffered solution (PBS) and kept at 4 °C before use.

Application of α-AMGO microreactors for the α-glucosidase inhibitors screening

The typical screening process of this method is demonstrated in Figure 1 (B). α-AMGO microreactors (20.00 mg) and *Dioscorea opposita* Thunb. peel extract (solution S0) extracted as reference22 were incubated and shaken in a vortex oscillator beaker under 37 °C for 2 h. Then carefully removing of the supernatant by magnetic separation, the α-AMGO microreactors were washed several times

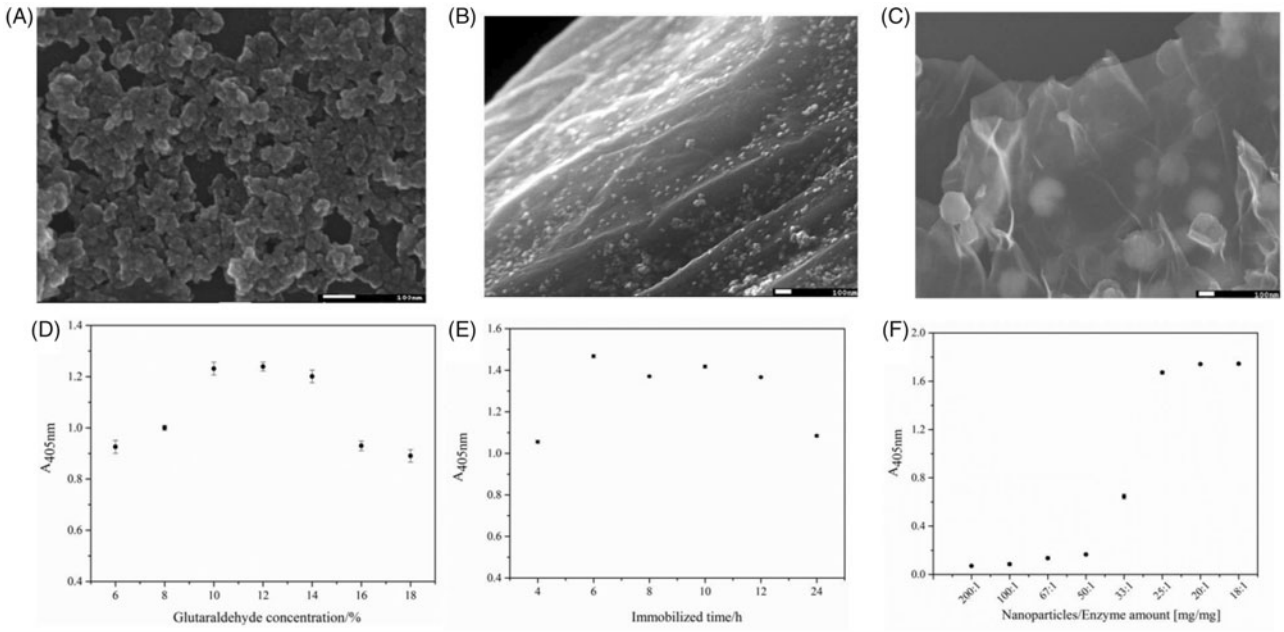

Figure 3. Influence of different proportions of $FeCl_3{\cdot}6H_2O$ to GO (50:1 (A), 5:1 (B), 2.5:1 (C)), glutaraldehyde (crosslinking agent) concentration (D), immobilised time (E) and enzyme (α-glucosidase) amount (F) on the immobilised enzyme absorbance values ($A_{405\,nm}$).

with PBS buffer solution until washed solutions did not exist free α-glucosidase. Finally, the α-AMGO microreactors reacted with 1 ml 90% acetonitrile (v/v) for three times and the eluent solutions were carefully saved as solution S1. The rGO@Fe_3O_4 (AMGO) nanocomposite were employed to be negative control for the inhibitors screening to remove the nonspecific binding and the final eluent solution was named as solution S2. The inhibitor screening capacity (ISC) with α-AMGO microreactors was calculated by the following equation:

$$ISC(\%) = \frac{[C_1]-[C_2]}{[C_0]} \times 100\%$$

Where the ligand concentration in solution S1, S2 were referred as $[C_1]$, $[C_2]$, with $[C_0]$ being all of ligand concentration in solution S0. All of solutions S0, S1 and S2 were filtrated through 0.22 μm filter membrane when HPLC-MS system analyzed.

Results and discussion

Characterisation of AMGO nanocomposite and α-AMGO microreactors

As shown in Figure 2, the as-prepared AMGO nanocomposite were detailedly characterised by FT-IR, XRD, TEM, SEM, magnetic properties and the α-AMGO microreactors were studied by SEM. The synthesis reaction mechanism was featured by nucleophilic substitution of carboxyl groups in GO and hydroxyl in Fe_3O_4[23] in Figure 1. FT-IR spectra of the GO (1), amine-functionalised Fe_3O_4 (NH_2-Fe_3O_4) (2), AMGO (3) were shown in Figure 2(A). The GO sheet showed characteristic adsorption bands with the 1735 cm^{-1} (carboxyl C = O), 1623 cm^{-1} (aromatic C = C), 1400 cm^{-1} (carboxyl C–O), 1219 cm^{-1} (epoxy C–O), 1050 cm^{-1} (alkoxy C–O groups) and 3409 cm^{-1} (hydroxy –OH group)[21–26]. For NH_2-Fe_3O_4, the peaks were observed at 2917, 2848, 1488 and 890 cm^{-1}, 585 cm^{-1} (Fe–O functional groups), indicating that the Fe_3O_4 nanoparticle were successfully functionalised with amino groups[24–30]. After the solvothermal reaction of GO with 1,6-hexanediamine, the GO peak at 1400 cm^{-1} totally vanished, and the intensity of peak at 1735 cm^{-1} decreased obviously and the appearance of two new characteristic peaks (-CONH amide band I, NH amide band II) at 1640 and 1562 cm^{-1}, respectively, in AMGO indicated the effective chemical interaction between alkyl-amines and GO by the formation of amide linkages[31], and the characteristic peaks (2917, 2848, 1488 and 890 cm^{-1}) of NH_2–Fe_3O_4 were also found in AMGO. Thus, it was concluded that AMGO was synthesised successfully from above results.

The XRD patterns of GO (1), NH_2-Fe_3O_4 (2) and AMGO nanocomposite (3) were presented in Figure 2(B). GO showed a sharp peak centered at $2\theta = 10.3°$ (002), indicating the presence of the oxygen functional groups[30,32]. The diffraction peaks (2θ) of the as-synthesised NH_2-Fe_3O_4 particles at 18.2, 30.1, 35.6, 43.0, 53.5, 57.0, 62.5 were ascribed to the (111), (220), (311), (400), (422), (511), (440) of the magnetite Fe_3O_4, which were in accord with pure spinel Fe_3O_4 (JCPDS no. 89–3854)[27,30]. The characteristic diffraction peaks of GO at $2\theta = 10.3°$ had been mostly replaced by a low and broad peaks of AMGO around $2\theta = 21.3°$, which indicated that GO was reduced to rGO in the reaction process[32]. The as-prepared AMGO nanocomposite presented all diffraction peaks of the NH_2-Fe_3O_4 particles and rGO and the XRD results revealed their high crystallinity.

The magnetic properties of AMGO nanocomposite were observed at 25 °C by MPMS3 Magnetic properties system that was illustrated in Figure 2(C). The AMGO nanocomposite dispersed well in water and could be drawn to the sidewall with magnet in a few minutes and the saturation magnetisation was 0.25 emu/g from the plots of magnetisation versus field.

As shown in Figure 2(D–F), TEM of GO (D), SEM of AMGO (E) and α-AMGO microreactors (F) images were observed. GO exhibited irregular sheets with some wrinkles which provided a large surface area and many oxygen functional groups. NH_2-Fe_3O_4 nanoparticle were strongly anchored on the surface of rGO sheets with a applicable density (shown in Figure 3(E)), implying the strong interaction between NH_2-Fe_3O_4 particles and rGO sheets. The successful construction of α-AMGO microreactors was revealed by comparing the SEM images of AMGO nanocomposite before (E) and after conjugation (F). The morphology of AMGO nanocomposite were nearly smooth and few aggregation and the surface (F) was slightly coarse and obviously aggregated after the conjugation step, which demonstrated the successful construction of α-AMGO microreactors.

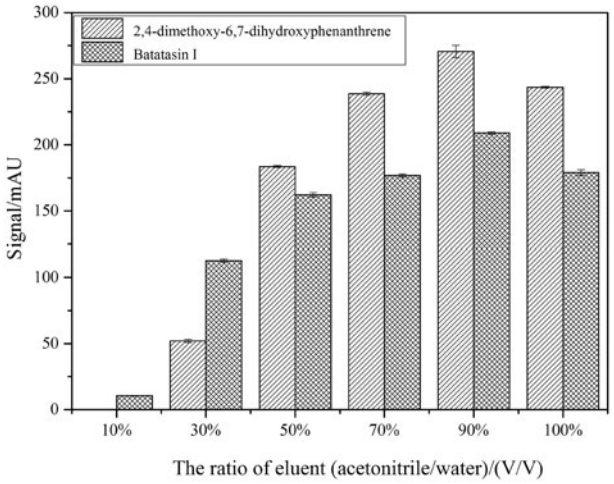

Figure 4. Effect of different proportions of denature solvent (acetonitrile-water (V/V), 10%, 30%, 50%, 70%, 90%, 100%).

Improvement of microreactors construction procedure

Proportion of $FeCl_3{\cdot}6H_2O$ to GO

The synthesis of AMGO nanocomposite was studied by controlling the proportion of $FeCl_3{\cdot}6H_2O$ to GO (w/w) with different ratios (50:1, 5:1, 2.5:1) in Figure 3(A–C, respectively) by SEM. As shown in Figure 3(C), it exhibited clearly irregular sheets with some wrinkles of GO and homogeneous NH_2-Fe_3O_4 nanoparticle (average particle size was 20 nm). However, if the amount of $FeCl_3{\cdot}6H_2O$ was increased, the surface of irregular sheets was entirely filled with nanoparticle and the wrinkles was aggregated seriously as shown in Figure 3(A,B). When the amount of $FeCl_3{\cdot}6H_2O$ was decreased, good morphology of AMGO could be obtained, however, their magnetic properties decreased, which would cause difficulties in subsequent magnetic separation of samples. Clearly, the aggregation was improved obviously with the increasing amount of GO. When the proportion of $FeCl_3{\cdot}6H_2O$ to GO (w/w) was 2.5:1, the large surface area and modest magnetic properties of AMGO nanocomposite made them appropriate to be a support for the enzyme immobilisation. Consequently, the proportion of (2.5:1) was selected for the following experiment.

Crosslinking agent concentration

Glutaraldehyde (GA) was used as crosslinking agent in this construction procedure, but it also was a denaturing reagent in high concentration, thus appropriate crosslinking agent concentration was an important optimisation parameters. Different GA concentrations (v/v, from 6 to 18%) were chosen to observe the relation between glutaraldehyde concentration and the *p*NP absorbance at 405 nm. As shown in Figure 3(D), the A_{405} values raised with different crosslinking agent concentrations increasing and then reached maximum value at 10%, then the absorbance in 405 nm remained until the concentration was 14%, but the absorbance values decreased when the concentration was between 14 and 18%. Obviously, when the crosslinking agent concentration was at low, the aldehyde process of AMGO nanocomposite was inadequate resulting in little α-glucosidase immobilised on the nanocomposite. When the glutaraldehyde concentration increased, the aldehyde process completed and the immobilised enzyme amount reached saturation status, but the active groups (–CHO) in the surface of AMGO could be multi-side combined or covered with each other in high crosslinking agent concentration leading to partial inactivation of α-glucosidase, so the A_{405nm} absorbance decreased. Therefore, 10% glutaraldehyde was selected as the optimum crosslinking agent concentration.

Reaction time

Different immobilisation times were investigated for α-glucosidase microreactors construction with the optimum crosslinking agent concentration. From Figure 3(E), it could be found that 6 h was the optimised reaction time. When the immobilised time was less than 6 h, the immobilised procedure was incomplete and inadequate. The absorbance decreased gradually with the immobilised time increasing when the time was more than 6 h. The reason might be that the conformation changes and partial inactivation of α-glucosidase due to the vibration at a long time. Hence, the optimised reaction time was chosen as 6 h.

Enzyme amount

In order to find out the relation between the *p*NP absorbance ($A_{405\,nm}$) and the amount of enzyme, different ratios (w/w) of AMGO to α-glucosidase with proportions (200:1, 100:1, 67:1, 50:1, 33:1, 25:1, 20:1, 18:1) was studied in Figure 3(F). As was shown that the $A_{405\,nm}$ values gradually increased with the increasing of α-glucosidase amount, and until the proportions was 25:1, the A_{405nm} value of *p*NP remained unchanged. The reason could be that the immobilisation procedure was inadequate in low proportion of AMGO to enzymes (w/w) resulting in less pNPG was hydrolyzed, and when the ratio was more than 25:1, it could be found that the absorbance value ($A_{405\,nm}$) changed unobviously due to its saturation. Thus, the optimised α-glucosidase amount was the proportion of 25:1. The immobilised amount of α-glucosidase on enzyme microreactors surface was about 40 μg α-glucosidase/mg nanocomposite that was about five times of the amount in our previous work[19]. The large immobilisation enzyme amount could obviously improve the application of α-glucosidase microreactors for inhibitors screening from natural products.

Identification of α-glucosidase inhibitors with α-glucosidase microreactors

α-AMGO microreactors were employed to screen the ligand from Chinese Yam peel extract and different proportions of denaturing solvent were also observed to separate the ligand that specifically bound to the α-AMGO microreactors in this work. As shown in Figure 4, different proportions of denature solvent (acetonitrile-water (V/V), 10, 30, 50, 70, 90, 100%) were studied by comparing the peak signal of specifically bound inhibitors to screen the optimised denaturing solvent. From the peak signals trend of two inhibitors in Figure 4, the 90% (V/V) acetonitrile-water had the optimum effect of the solubility and the separation efficiency of the screening ligand. Figure 5 showed the typical HPLC chromatograms of the solutions S0 (a), the eluent solutions S1 (the first eluent (b), the second eluent (c) and the third eluent (d)) as well with the blank eluent S2 (e) and the necessary MS^1/MS^2 informations (1, 2, 3, 4) of the specifically bound inhibitors to α-AMGO microreactors. The HPLC-MS conditions were as reference22: chromatographic column: COSMOSIL 5C18-PAQ (4.6 ID ×250 mm, 5 μm); A HPLC gradient program: solvent A (methanol) and solvent B (water), 60% A at 0–6 min, 60–50% A at 6–8 min, 50–70% A at 8–15 min and 70% A at 15–30 min, flow rate: 1 ml min^{-1}, column temperature: 30 °C, injection volume: 5 μL, and detected wavelength: 274 nm; the capillary voltage was 4.5 kV; the endplate

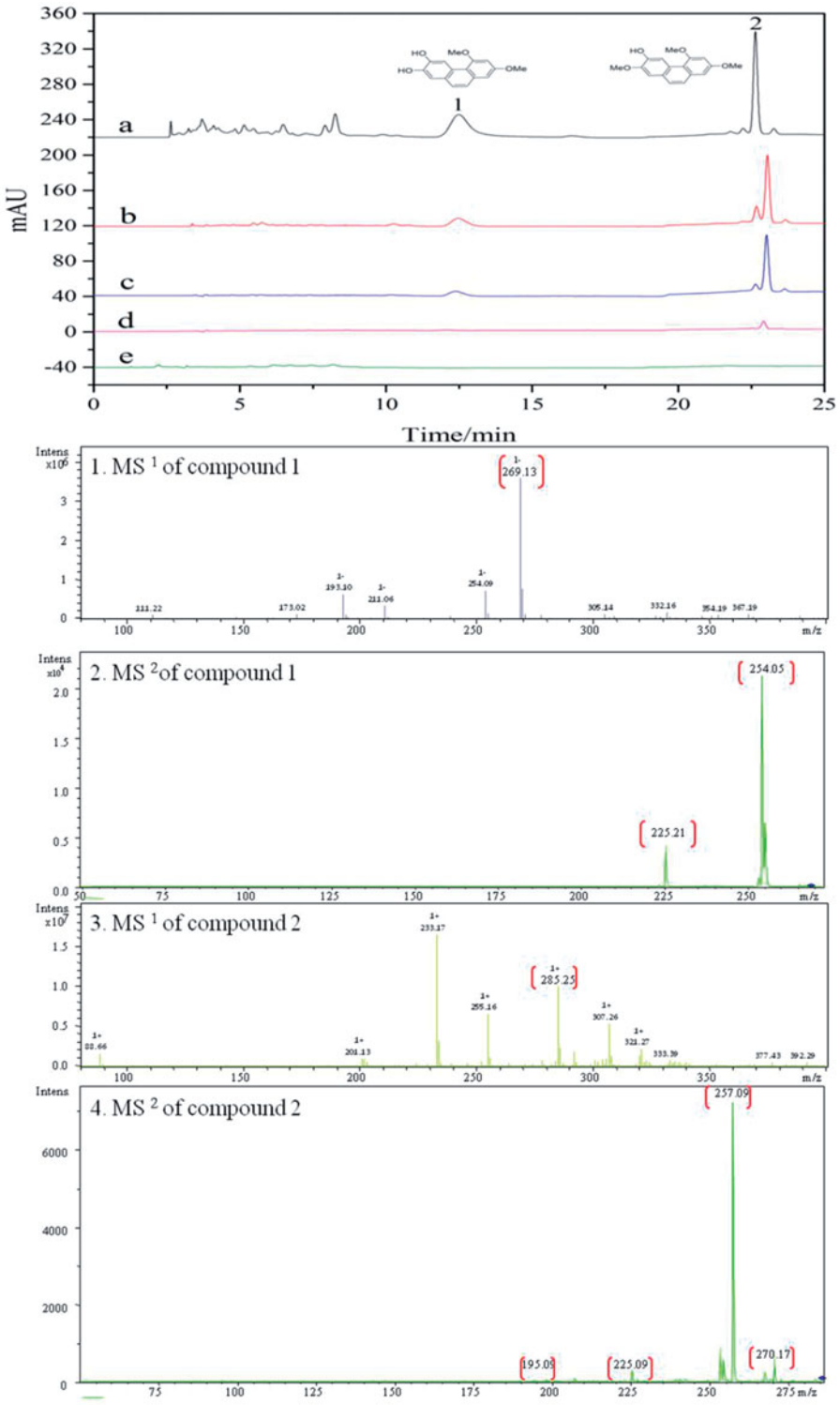

Figure 5. Typical HPLC chromatograms of solutions S0 (a), the eluent solutions S1 (the first eluent (b), the second eluent (c) and the third eluent (d)) and the blank eluent S2 (e) and the necessary MS^1/MS^2 informations (1, 2, 3, 4) of the specifically bound inhibitors to α-AMGO microreactors. The inset were the chemical structurals of trapped ligands. Conditions were as reference 22.

Table 1. The immobilisation amount and binding capacities of α-glucosidase by the enzyme microreactors construction to screen potential ligands from complex natural resources.

	This work	Reference[17]	Reference[22]
immobilisation amount (μg/mg)	40	—	8.04
binding capacities (%)	35.6%/68.2%	14.04%/12.77%	26.7%/15.6%

offset voltage was 500 V; the nebulizer pressure source was set at 15 psi; the flow rate of dry gas was 8 L min^{-1}; and the dry temperature and vaporiser temperature were 220 °C and 300 °C. Comparing with the *Dioscorea opposita* Thunb. peel extract and blank solution, two ligands named as 2,4-trimethoxy-6,7-dihydroxyphe-nanthrene, Batatasin I (structures were shown in the top of Figure 5), were found to be specifically bound to the α-AMGO

microreactors. It could be seen that, after three times' elution, the bound two inhibitors were almost completely washed off from the α-AMGO microreactors, which suggested that the components strongly and stably bound with α-glucosidase microreactors. Figure 5 (1, 2, 3, 4) displayed the useful mass spectral characteristics of two ligand. The immobilised amount and binding capacities of α-glucosidase were shown in Table 1. when the α-AMGO microreactors was employed as baits for inhibitors fishing, the immobilised amount and binding capacities were about more than five times, one and a half, and four times higher, respectively. The reason might be that the composition of GO with Fe_3O_4 not only increased the large active groups for the enzyme immobilisation, but also maintained excellent magnetic separation ability. And two specifical bound ligand were latent candidates for the antidiabetic agents development by the observing the inhibition assay[20,22]. Thus, the construction idea of α-glucosidase microreactors based on AMGO was an effective, feasible and sensitive method for the specifical separation of biological active compounds from the complex nature products.

Conclusions

In short, a typical one-pot solvothermal method was exploited to prepare amine-functionalised magnetite nanocomposite containing rGO and Fe_3O_4 and the nanocomposite were selected as support matrix for the covalent immobilisation of α-glucosidase to successfully construct the enzymatic microreactors. The data presented in this paper provided strong evidence that the rGO@Fe_3O_4 nanocomposite exhibited significantly higher immobilisation efficiency and binding capacities that could be employed as supports for the enzyme microreactors construction to screen the potential ligand from natural product resources.

Disclosure statement

No potential conflict of interest was reported by the authors.

Funding

We are grateful for financial support from the National Natural Science Foundation of China [21705033] and the Natural Science Foundation of Henan Provincial Science and Technology Department [162300410043, 182102410077].

References

1. Boath AS, Stewart D, McDougall GJ. Berry components inhibit α-glucosidase in vitro: synergies between acarbose and polyphenols from black currant and rowanberry. Food Chem 2012;135:929–36.
2. Mohan S, Eskandari R, Pinto BM. Naturally occurring sulfonium-ion glucosidase inhibitors and their derivatives: a promising class of potential antidiabetic agents. Acc Chem Res 2014;47:211–25.
3. Yin Z, Zhang W, Feng F, et al. α-Glucosidase inhibitors isolated from medicinal plants. Food Sci Human Wellness 2014;3:136–74.
4. Chiba S. Molecular mechanism in alpha-glucosidase and glucoamylase. Biosci Biotechnol Biochem 1997;61:1233–9.
5. Rengasamy KR, Aderogba MA, Amoo SO, et al. Potential antiradical and alpha-glucosidase inhibitors from Ecklonia maxima (Osbeck) Papenfuss. Food Chem 2013;141:1412–15.
6. Secil O, Suna T, Burcu O, et al. Inhibition of alpha-glucosidase by aqueous extracts of some potent antidiabetic medicinal herbs. Prep Biochem Biotechnol 2005;35:29–36.
7. Matsumura T, Kasai M, Hayashi T, et al. α-glucosidase inhibitors from paraguayan natural medicine, nangapiry, the leaves of Eugenia Uniflora. Pharm. Biol 2000;38:302–7.
8. Zhang L, Bai B, Liu XH, et al. α-Glucosidase inhibitors from Chinese Yam (*Dioscorea opposita* Thunb.). Food Chem 2011;126:203–6.
9. He J. Bioactivity-guided fractionation of pine needle reveals catechin as an anti-hypertension agent via inhibiting angiotensin-converting enzyme. Sci Rep 2017;7:8867.
10. Kaufmann K, Simmons L, Herrmann J, et al. Activity-guided screening of bioactive natural compounds implementing a new glucocorticoid-receptor-translocation assay and detection of new anti-inflammatory steroids from bacteria. Biotechnol Lett 2013;35:11–20.
11. Li Y, Lu Q, Tan S, et al. Bioactivity-guided isolation of antioxidant and anti-hepatocarcinoma constituents from *Veronica ciliata*. Chem Cent J 2016;10:27.
12. Wang SY, Tseng CP, Tsai KC, et al. Bioactivity-guided screening identifies pheophytin a as a potent anti-hepatitis C virus compound from *Lonicera hypoglauca* Miq. Biochem Biophys Res Commun 2009;385:230–5.
13. Yu JG, Liu P, Duan JA, et al. Itches-stimulating compounds from *Colocasia esculenta* (taro): bioactive-guided screening and LC-MS/MS identification. Bioorg Med Chem Lett 2015;25:4382–6.
14. Sun S, Kadouh HC, Zhou K, Zhu WJ. Bioactivity-guided isolation and purification of α-glucosidase inhibitor, 6-O-D-glycosides, from Tinta CÃO grape pomace. J Funct Foods 2016;23:573–9.
15. Qing LS, Xue Y, Zheng Y, et al. Ligand fishing from *Dioscorea nipponica* extract using human serum albumin functionalized magnetic nanoparticles. J Chromatogr A 2010;1217:4663–8.
16. Zhu YT, Jia YW, Liu YM, et al. Lipase ligands in *Nelumbo nucifera* leaves and study of their binding mechanism. J Agric Food Chem 2014;62:10679–86.
17. Tao Y, Zhang Y, Cheng Y, Wang Y. Rapid screening and identification of α-glucosidase inhibitors from mulberry leaves using enzyme-immobilized magnetic beads coupled with HPLC/MS and NMR. Biomed Chromatogr 2013;27:148–55.
18. Li HT. Preliminary study on the 5-lipoxidase inhibitory activities of Chinese yam (*Dioscorea opposita* Thunb.) [Dissertation]. Kaifeng: Henan University, 2015.
19. Liu XH, Hu WP, Bai B, et al. A method for extracting Batatasin from *Dioscorea opposita* Thunb. Chinese Patent No. ZL201410083342.4[P]. 2016-8-17.
20. Hu WP, Cao GD, Zhu JH, et al. Naturally occurring Batatasins and their derivatives as α-glucosidase inhibitors. RSC Adv 2015;5:82153–8.
21. Zhao G, Wang J, Li Y, et al. Enzymes immobilized on superparamagnetic Fe_3O_4@Clays nanocomposites: preparation, characterization, and a new strategy for the regeneration of supports. J Phys Chem C 2011;115:6350–9.
22. Zhang SS, Wu DD, Li H, et al. Rapid identification of α-glucosidase inhibitors from *Dioscorea opposita* Thunb. peel extract by enzyme functionalized Fe_3O_4 magnetic nanoparticles coupled with HPLC-MS/MS. Food Funct 2017;8:3219–27.
23. Lai L, Chen L, Zhan D, et al. One-step synthesis of NH_2-graphene from in situ, graphene-oxide reduction and its improved electrochemical properties. Carbon 2011;49:3250–7.

24. Chhetri S, Samanta P, Murmu NC, et al. Effect of dodecyal amine functionalized graphene on the mechanical and thermal properties of epoxy-based composites. Miner Deposita 2016;50:1031.
25. Song JG, Wang XZ, Chang CT. Preparation and characterization of graphene oxide. J Nanomater 2014;2014:276143.
26. Zhao CY, Ma LJ, You JM, et al. EDTA- and amine-functionalized graphene oxide as sorbents for Ni(II) removal. Desalin Water Treat 2016;57:8942–10.
27. Wang LY, Bao J, Wang L, et al. One-pot synthesis and bioapplication of amine-functionalized magnetite nanoparticles and hollow nanospheres. Chem Eur J 2006;12: 6341–6347.
28. Boruah PK, Sharma B, Karbhal I, et al. Ammonia-modified graphene sheets decorated with magnetic Fe_3O_4 nanoparticles for the photocatalytic and photo-Fenton degradation of phenolic compounds under sunlight irradiation. J Hazard Mater 2017;325:90.
29. Zhang JL, Srivastava RS, R, Misra DK. Core-shell magnetite nanoparticles surface encapsulated with smart stimuli-responsive polymer: synthesis, characterization, and LCST of viable drug-targeting delivery system. Langmuir 2007;23:6342–6351.
30. Wu QH, Feng C, Wang C, Wang Z. A facile one-pot solvothermal method to produce superparamagnetic grapheme-Fe_3O_4, nanocomposite and its application in the removal of dye from aqueous solution. Colloids Surf B 2013;101:210–214.
31. Ma L, Wang GJ, Dai JF. Influence of structure of amines on the properties of amines-modified reduced graphene oxide/polyimide composites. J Appl Polym Sci 2016;133:43820.
32. Ma CQ, Yang KY, Wang LL, Wang X. Facile synthesis of reduced graphene oxide/Fe_3O_4 nanocomposite film. J Appl Biomater Funct Mater 2017;15(Suppl. 1):e1–e6.